the plant journal

SEB SOCIETY FOR EXPERIMENTAL BIOLOGY

The Plant Journal (2020) **102,** 18–33 doi: 10.1111/tpj.14608

Arabidopsis *PIC30* encodes a major facilitator superfamily transporter responsible for the uptake of picolinate herbicides

Praveen K. Kathare[1,3], Sunethra Dharmasiri[1], Eric D. Vincill[2], Pratyush Routray[2], Idrees Ahmad[1], Daniel M. Roberts[2] and Nihal Dharmasiri[1,*]

[1]*Department of Biology, Texas State University, 601 University Drive, San Marcos, TX 78666,*

[2]*Department of Biochemistry, and Cellular and Molecular Biology, University of Tennessee, Knoxville, Tennessee, 37996, and*

[3]*Department of Molecular Biosciences, University of Texas, Austin TX 78712, USA*

Received 4 December 2018; revised 27 September 2019; accepted 15 October 2019; published online 11 November 2019.
*For correspondence (e-mail nihal@txstate.edu).

SUMMARY

Picloram is an auxinic herbicide that is widely used for controlling broad leaf weeds. However, its mechanism of transport into plants is poorly understood. In a genetic screen for picloram resistance, we identified three Arabidopsis mutant alleles of *PIC30* (*PICLORAM RESISTANT30*) that are specifically resistant to picolinates, but not to other auxins. *PIC30* is a previously uncharacterized gene that encodes a major facilitator superfamily (MFS) transporter. Similar to most members of MFS, PIC30 contains 12 putative transmembrane domains, and PIC30-GFP fusion protein selectively localizes to the plasma membrane. *In planta* transport assays demonstrate that PIC30 specifically transports picloram, but not indole-3-acetic acid (IAA). Functional analysis of *Xenopus laevis* oocytes injected with PIC30 cRNA demonstrated PIC30 mediated transport of picloram and several anions, including nitrate and chloride. Consistent with these roles of PIC30, three allelic *pic30* mutants are selectively insensitive to picolinate herbicides, while *pic30-3* is also defective in chlorate (analogue of nitrate) transport and also shows reduced uptake of $^{15}NO_3^-$. Overexpression of *PIC30* fully complements both picloram and chlorate insensitive phenotypes of *pic30-3*. Despite the continued use of picloram as an herbicide, a transporter for picloram was not known until now. This work provides insight into the mechanisms of plant resistance to picolinate herbicides and also shed light on the possible endogenous function of PIC30 protein.

Keywords: auxin, synthetic auxins, herbicides, picloram, major facilitator superfamily, picloram transport, anion transport, *Arabidopsis thaliana*.

INTRODUCTION

The plant hormone auxin essentially influences all aspects of plant growth and development including root and shoot growth, organ patterning and flower development (Hagen and Guilfoyle, 2002). While an optimal concentration of auxin stimulates growth and development, hyperaccumulation of auxin promotes abnormal metabolic activities leading to the death of the plant (Grossmann *et al.*, 2001). Based on this property, several synthetic auxinic chemicals including 2,4-D (2,4-dichlorophenoxyacetic acid), dicamba, and picloram, have been developed as herbicides. Whereas 2,4-D and dicamba are traditionally used in agriculture, picloram is extensively used for non-agricultural purposes, including forest and rangeland management (Evans and Norris, 1986; Mithila *et al.*, 2011). Auxinic chemicals specifically act against a broad range of dicots (McSteen, 2010), and as a result, their use is limited to eradicating broad leaf weeds from monocot crops. One of many ways in which this problem can be solved is to create herbicide resistant crop varieties. However, our current knowledge on the mechanism of herbicide transport and its subsequent signalling mechanism is very limited. Among the synthetic auxinic herbicides presently in use, details of the molecular mechanisms of action and transporter proteins responsible for the cellular influx and efflux are known only for 2,4-D (Ito and Gray, 2006; Calderon-Villalobos *et al.*, 2012). Although some of the genes involved in picloram response have been described previously (Walsh *et al.*, 2006; Prigge *et al.*, 2016), none of the

© 2019 The Authors
The Plant Journal © 2019 John Wiley & Sons Ltd

proteins involved in the transport of picloram has been characterized so far. Therefore, identifying the genes involved in picloram transport and signalling may help us to understand the genetic basis of picloram action, and to potentially use this knowledge to dissect the mechanisms of picloram resistance in weeds and for the generation of genetically modified picloram tolerant plants. This knowledge also opens possibilities for developing plant remedies to remove picloram residues from soil.

Previous work has shown that synthetic auxin, 2,4-D is transported by ATP-binding cassette transporter protein, which also transports natural auxin precursor indole-3-butyric acid (IBA), but not indole-3-acetic acid (IAA) (Ruzicka *et al.*, 2010). Another study recently showed that major facilitator superfamily (MFS) transporter ZIFL1.1 plays an indirect role in polar IAA transport through modulating the abundance of PIN2 auxin effluxer (Remy *et al.*, 2013). As picloram is a synthetic substrate, its transport into plant cells must occur as a secondary substrate of a native transporter mechanism. MFS is one of the largest families of membrane transporter proteins found in almost all types of organisms on earth (Pao *et al.*, 1998). Most members of this family contain 12 transmembrane domains and are localized to either the plasma membrane or organelle membranes (Marger and Saier, 1993; Haydon and Cobbelt, 2007; Peng *et al.*, 2011; Ricachenevsky *et al.*, 2011). During the last decade, extensive research has been done to understand the cellular functions of MFS proteins and their physiological implications. In Arabidopsis, members of this superfamily have been implicated in the transport of a wide variety of substrates, including hormones like auxin and ABA (Kanno *et al.*, 2012; Remy *et al.*, 2013; Leran *et al.*, 2014; Chiba *et al.*, 2015), nutrients such as nitrate and sugars (Reinders *et al.*, 2005; Büttner, 2007; Krouk *et al.*, 2010; Wang and Tsay, 2011; Leran *et al.*, 2014), and various heavy metal ions (Haydon and Cobbett, 2007; Peng *et al.*, 2011). Because of their abilities to transport many different classes of substrates, they are considered important players in plant growth and development. Despite the extensive knowledge on MFS transporters, the individual functions of most members of the MFS have yet to be determined.

In this study, we have characterized Arabidopsis *PIC30*, for which three independent allelic mutants were identified in a genetic screen to isolate picloram-insensitive mutants. *pic30* mutants are semidominant, and are selectively insensitive to picolinate herbicides, but not to other auxinic chemicals such as indole-3-acetic acid (IAA) or 2,4-D. *PIC30* encodes a MFS transporter protein. Moreover, we demonstrate that PIC30 is a plasma membrane localized anion transporter that transports several anions, including nitrate and picloram.

RESULTS

Mutation in *pic30* confers insensitivity against auxinic herbicide picloram

Ethyl methanesulfonate (EMS) mutagenized Arabidopsis seeds were screened for insensitivity of primary root growth to 10 μM picloram. Three of the mutants identified based on this mutant screen were mapped to the same genetic window between the genes *At2g39110* and *At2g39260* to a region of 73 kb of the chromosome 2. Sequence analysis of the genes in this genetic window showed that all three mutants were allelic to the *At2g39210* gene. These mutants were subsequently referred to as *pic30-1*, *pic30-2*, and *pic30-3*. Phylogenetic analysis revealed that *PIC30* grouped with a subfamily of proteins with two conserved domains. It is a member of the MFS domain in its NH_2– and COOH– termini, respectively (www.arabidopsis.org). Mutations in both *pic30-1* and *pic30-3* were found to be within the nucleotide-binding oligomerization domain (NOD). The mutation in *pic30-1* is a C→T ($C^{392}T$) change in its first exon resulting in an amino acid substitution from serine to leucine ($S^{131}L$). The mutation in *pic30-2* is a domain (Figure 1a and Supporting Information Figure S1b). The mutation in *pic30-3* is a G→A ($G^{698}A$) change in its intron, altering the conserved 'G' within the 3 splice site consensus sequence (Figure 1a).

Of the three *pic30* allelic mutants, the primary root growth of *pic30-3* was slower than that of the wild type, *pic30-1*, and *pic30-2* (Figure 1b, left panel). All three mutants were highly insensitive to picloram during seedling and adult stages as assessed by root growth inhibition assays on picloram (Figure 1b, right panel) and response to foliar treatment of picloram, respectively (Figure 1c). Moreover, picloram-insensitive root growth phenotype in *pic30* mutants was inherited as a semidominant trait (Figure 1d).

pic30 mutants are selectively insensitive to picolinate class of synthetic herbicides

As *pic30* allelic mutants were isolated in picloram-insensitive screening, primary root growth response was tested on incremental doses of picloram. As shown in Figure 2a, root growth of all three *pic30* mutants was found to be highly insensitive to elevated levels of picloram. To test whether these mutants exhibited insensitivity to other auxins, root growth responses were also compared on the natural auxin IAA and the synthetic auxins 2,4-D, 1-NAA and aminopyralid. It was observed that root growth of *pic30* mutants were also insensitive to aminopyralid (Figure 2b) but not to IAA, 2,4-D or 1-NAA (Figure 2c–e). As both picloram and aminopyralid belong to the picolinate class of synthetic herbicides, it shows that mutations in *pic30* selectively confer insensitivity against the picolinate class of auxinic herbicides.

© 2019 The Authors
The Plant Journal © 2019 John Wiley & Sons Ltd,

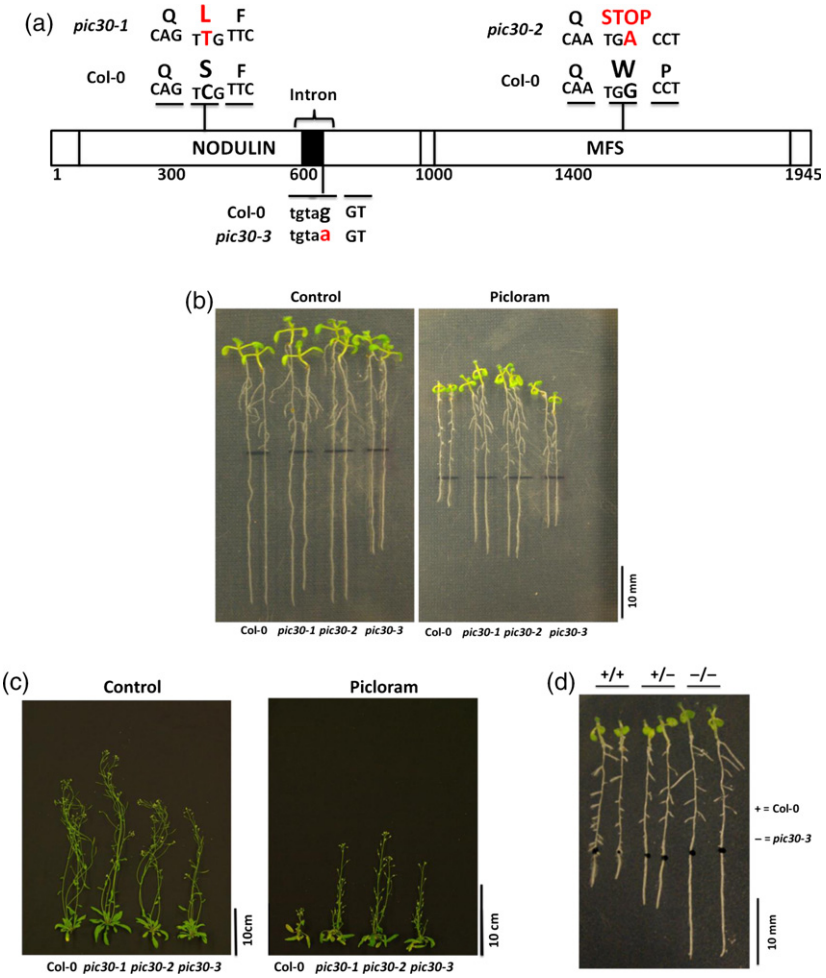

Figure 1. *pic30* mutants are insensitive to picloram.
(a) Schematic representation of *pic30* mutations. The *PIC30* gene contains sequences encoding an NH_2-terminal NODULIN (NOD-) domain and a COOH-terminal MFS domain. *pic30-1* is a missense mutation in the NOD domain, *pic30-2* is a non-sense mutation in the MFS domain, and *pic30-3* is a splice site mutation. Mutations in nucleotide sequence and related changes in amino acid residues are given in bold letters.
(b) The primary root growth of *pic30-1, pic30-2,* and *pic30-3* mutants is insensitive to picloram. (c) All three *pic30* allelic mutants are insensitive to foliar application of picloram. (d) Picloram-insensitive phenotype of *pic30* mutants inherits as a semidominant trait (only *pic30-3* is shown). For root growth assay, 4-day-old seedlings were transferred onto the ATS medium (for mock treatment) or ATS with 12.5 μM picloram. After 4 days of incubation, images were acquired using NIKON SMZ1500 stereomicroscope. Black lines on the plates indicate the position of the root tip soon after the transfer of seedlings to treatment plates. For foliar picloram application, *c.* 3-week-old plants grown in pots were homogenously sprayed with 200 g/ha of picloram. Images were acquired 18 days after the treatment. For root growth assays 15–20 seedlings per genotype were used, while 20 plants per genotype were used for foliar application. Images were taken using representative seedlings from each genotype/treatment. Experiments were repeated three times with similar results.

To gain further insight into picolinate specific insensitivity of *pic30* mutant alleles, one of the three *pic30* mutant alleles, *pic30-3*, was crossed into auxin responsive reporter line *DR5::GFP*. When treated with different auxins, *DR5::GFP* expression in *pic30-3* was upregulated exclusively by IAA and 2,4-D but not by either picloram or aminopyralid (Figure 2f), further confirming picolinate specific insensitivity of the *pic30* mutant alleles.

pic30-3 mutation disrupts proper splicing

As the mutation in *pic30-3* disrupts the conserved nucleotide 'G' in the 3 splice site (Figure 1a), we hypothesized that the splicing of *pic30* transcript may be defective in the *pic30-3* mutant. To test this, a reverse transcriptase polymerase chain reaction (RT-PCR) was performed with *PIC30* specific primers using cDNA synthesized from total RNA isolated from wild type and *pic30-3* seedlings. Results indicated that *PIC30* primary transcript in *pic30-3* does not undergo splicing, resulting in a longer mature transcript compared with that of wild type (Figure S1c). Defective splicing introduces two premature in-frame stop codons in *pic30-3* (Figure S1d).

To test *PIC30* transcript levels in mutant lines, semiquantitative RT-PCR and quantitative real time-PCR (qRT-PCR) were performed using cDNA synthesized from total RNA isolated from seedlings of three mutant lines and wild

© 2019 The Authors

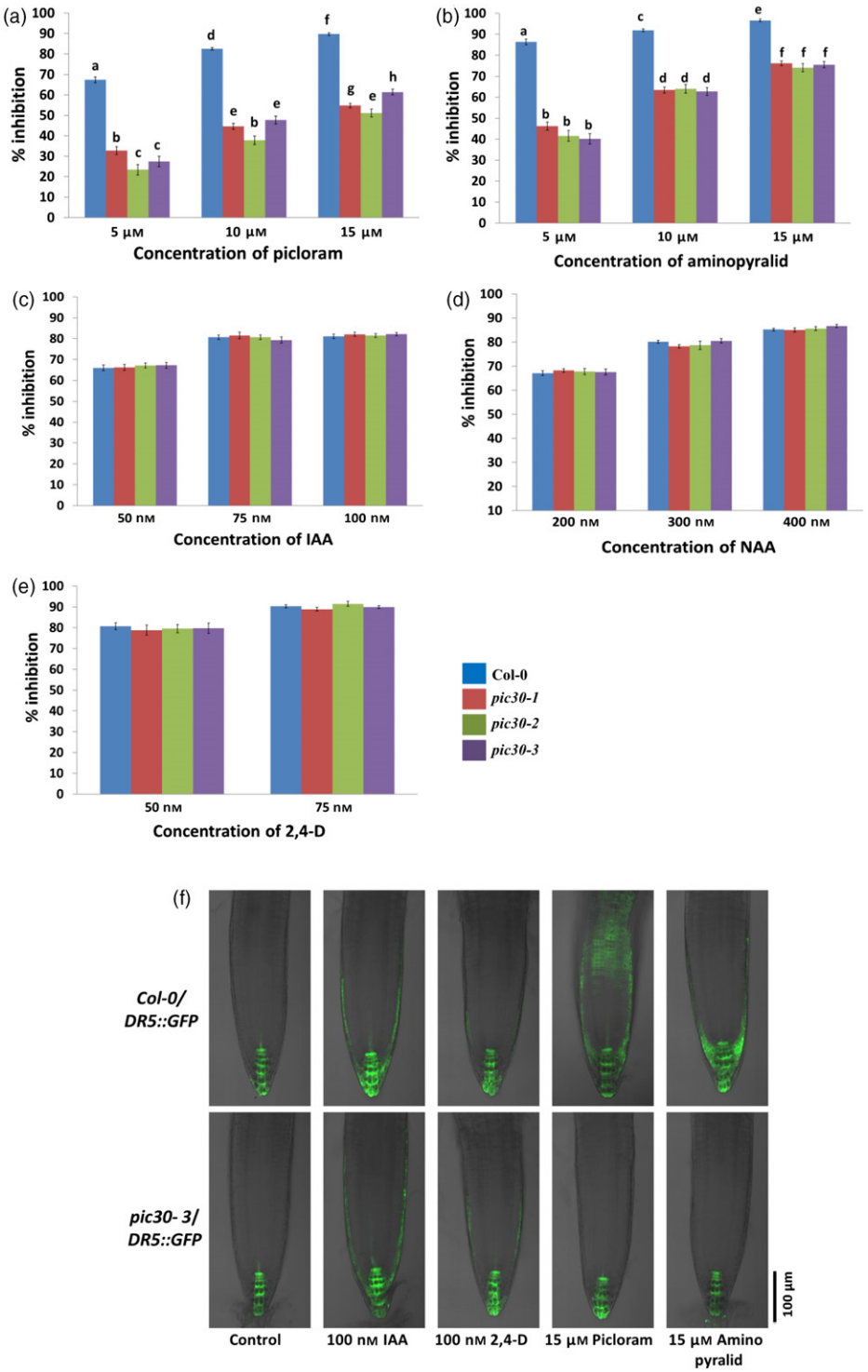

Figure 2. *pic30* mutants are selectively insensitive to picolinate class of auxinic herbicides.
The primary root growth of *pic30* mutants is insensitive to (a) picloram and (b) aminopyralid, but shows wild type sensitivity to (c) IAA, (d) 1-NAA and (e) 2,4-D. Four-day-old seedlings were transferred to ATS medium (control) or ATS containing indicated concentrations of different auxins and primary root lengths were measured after 4 days of incubation. Each data point reflects the mean percentage inhibition (MPI) (n = 15), and bars represent standard error of the mean (SEM). Statistical significance between the samples was determined by one-way ANOVA with Tukey's post-hoc test ($P < 0.01$). Statistical significance was indicated by different letters.
(f) Picloram and aminopyralid fail to induce *DR5::GFP* expression in *pic30-3,* while both IAA and 2,4-D induce *DR5::GFP* expression in a similar manner to wild type Col-0. Five-day-old seedlings were transferred on to ATS medium (control) or ATS medium with indicated concentrations of different auxinic chemicals. Confocal images were acquired 20 h after the incubation.

© 2019 The Authors

type. The data indicated that all three *pic30* mutant lines had significantly lower levels of transcript, with the lowest level in *pic30-3* compared with the wild type (Figure S2a, b). Therefore, due to its resemblance to a genetically null mutant, *pic30-3* was selected for most of the mutant characterizations presented here.

Several experimental points of evidence indicated that mutant transcripts with premature stop codons are subjected to degradation through nonsense-mediated mRNA decay (NMD) (Kurihara *et al.*, 2009), which is a conserved eukaryotic surveillance pathway involved in the destruction of aberrant mRNAs (Rayson *et al.*, 2012). To test whether the lower abundance of transcript in *pic30-3* is caused by the NMD pathway, we crossed *pic30-3* with one of the NMD mutants, *upf3-1* (Hori and Watanabe, 2005), and the *pic30-3 upf3-1* homozygous double mutant was obtained. qRT-PCR analysis showed that the transcript level was *c.* four-fold higher in *pic30-3upf3-1* double mutant compared with *pic30-3* (Figure S2c).

PIC30 localizes to the plasma membrane

Members of MFS superfamily predominantly contain 12 transmembrane domains and localize either to the plasma membrane or organelle membranes (Pao *et al.*, 1998). As PIC30 is a member of MFS superfamily, we hypothesized that PIC30 also localized to either the plasma membrane or to one or more organelle membranes. To determine the subcellular localization, PIC30 was fused in-frame with green fluorescent protein (GFP) to generate *35S*$_{pro}$*::PIC30-GFP* and was stably expressed in *pic30-3* (*PIC30-OX*). Analysis of the co-localization pattern of PIC30-GFP and membrane tracker dye FM4-64 revealed that PIC30-GFP was selectively localized to the plasma membrane in the root cells (Figure 3a–f). Moreover, a plasma membrane marker fused to mCherry protein (PM-RK; CD3-1007, Nelson *et al.*, 2007) was stably expressed in the *PIC30-OX* transgenic line. Again, PIC30-GFP was found to be co-localized with PM-RK in root cells (Figure S3).

Ectopic expression of *PIC30* complements picloram insensitivity of *pic30-3*

To determine if the wild type *PIC30* gene complements the picloram-insensitive root growth phenotype of the *pic30-3* mutant, several independent *PIC30*$_{Pro}$*::PIC30-HA* (*PIC30-HA*) and *35S*$_{pro}$*::PIC30-GFP* (*PIC30-OX*) transgenic lines expressing *PIC30-HA* (Figure S4a) and *PIC30-GFP* (Figure S4b,c) respectively were obtained.

To test for complementation of picloram insensitivity in *PIC30-HA* lines, a root growth inhibition assay was performed on medium containing increasing concentrations of picloram. It was observed that all four *PIC30-HA* lines complement picloram-insensitive root growth phenotype in *pic30-3* mutant background (Figure 4a). Similarly, *PIC30-OX* lines complemented picloram-insensitive root growth phenotype in *pic30-3* mutant (Figure 4b). Since *PIC30-OX* lines show extreme hypersensitivity to picloram at micromolar concentration, root growth inhibition was also assayed on 100 nM of picloram. As shown in Figure 4c, root growth of *PIC30-OX* lines was hypersensitive even at nanomolar concentrations of picloram compared with the wild type. Moreover, foliar treatment of adult plants with 100 g/ha of picloram also showed that *PIC30-OX* lines were hypersensitive to picloram (Figure S4d). By contrast, all four *PIC30-OX* lines displayed wild type sensitivity to both IAA and 1-NAA (Figure S4e,f).

Because overexpression of *PIC30* makes plants hypersensitive to picloram, we investigated whether overexpression of mutant *pic30* on the wild type background resulted in picloram insensitivity. Among the three *pic30* allelic mutants, only the *pic30-1* mutation resulted in the change of a single amino acid and, therefore, *pic30-1* was chosen for overexpression in wild type (Figure S4g). When independent homozygous lines of *pic30-1-OX* were tested on picloram, they displayed picloram-insensitive primary root growth (Figure 4d). These results explicitly indicated that plant sensitivity to picloram can be modulated through the *PIC30* gene.

***pic30-3* is defective in picloram uptake**

As PIC30 is categorized as a general substrate transporter, and mutations in *pic30* selectively conferred insensitivity to the picolinate class of auxinic herbicides, the possibility of picloram transport through PIC30 was investigated using radiolabelled ^{14}C-picloram. As roots are highly sensitive to picloram (Figure 1b), 15 mm sections from the root tips of 9-day-old seedlings were used for *in planta* picloram transport assays. Results showed that picloram uptake was significantly decreased in *pic30-3* compared with that of wild type root sections (Figure 5a), and this defect was found to be common to all three *pic30* mutant alleles (Figure S4h).

Our complementation root growth assay results indicated that picloram insensitivity of *pic30-3* can be restored by ectopic expression of *PIC30* (Figure 4a,b). To test whether this is due to restoration of picloram uptake ability, a transport assay was performed with two of the four *PIC30-HA* and *PIC30-OX* lines. Picloram uptake in *PIC30-HA #20* roots was found to be similar to that of wild type, while in *PIC30-HA #6* roots it was significantly higher than in the wild type (Figure 5b). Moreover, in two of the *PIC30-OX* lines, picloram uptake was found to be *c.* 28–35 times higher than that of wild type roots (Figure 5c).

To verify whether PIC30 is selective for picloram uptake, an *in planta* IAA transport assay was performed using

© 2019 The Authors

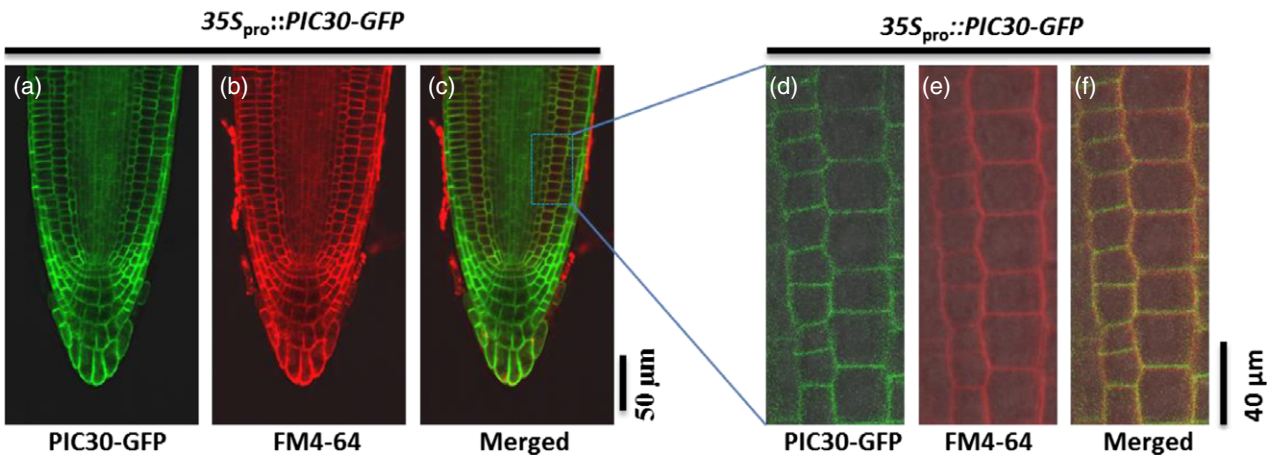

Figure 3. PIC30-GFP localizes to plasma membrane.
(a–f) PIC30-GFP preferentially localizes to plasma membrane in root cells. Five-day-old transgenic seedlings carrying *35S*$_{pro}$*::PIC30-GFP* were imaged using either a ×20 water immersion lens (a–c) or a ×60 oil immersion lens (d–f), using a confocal microscope.

radiolabelled ^{3}H-IAA with similar 15 mm apical root sections. In contrast with picloram uptake, no difference was detected in IAA uptake between wild type and *pic30-3* (Figure 5d), strongly indicating that PIC30 specifically transports picloram, but not the natural auxin IAA.

PIC30 is an inorganic anion transporter

The data above, and the fact that PIC30 is a MFS transporter, strongly suggested that it could serve as a direct transporter of picloram. To test this, PIC30 cRNA was generated and microinjected into *X. laevis* oocytes, and an uptake assay was performed using ^{14}C-picloram as a transport substrate. Microinjected oocytes showed expression of PIC30 after 3 days (Figure 6a) and exhibited a significantly higher uptake of picloram than control oocytes (Figure 6b), supporting a picloram transport function for PIC30.

Sequence and phylogenetic comparisons showed that PIC30 exhibits homology to two nodulin proteins in *Glycine max* (GmN70) and *Lotus japonicus* (LjN70). Previous work showed that these proteins exhibited transport selectivity for inorganic anions with a slight selective preference for nitrate over chloride, based on two-electrode voltage clamp recording (Vincill *et al.*, 2005).

To investigate the potential function of PIC30 as an anion transporter, *X. laevis* oocytes expressing PIC30 were assayed by two-electrode voltage clamp recording. Similar to GmN70 (Vincill *et al.*, 2005), oocytes expressing PIC30 exhibited both inward and outward currents in bath solutions containing a series of anions, and showing a preference for inorganic anions (Figure 6c) that was substantially higher than those observed with control oocytes. Taken together the radiolabelled uptake data from both oocyte and *in planta* showed that PIC30 possessed a picloram transport activity. Furthermore, similar to other orthologues in other plant species (GmN70 and LjN70) PIC30 also exhibited an inorganic anion transport activity for nitrate and chloride as well.

***pic30-3* mutant is insensitive to the nitrate analogue chlorate, and defective in nitrate uptake**

Based on the identification of an anion transport function for PIC30, including nitrate, in *X. laevis* oocytes (Figure 6c), it was hypothesized that mutations in *pic30* may affect its nitrate transporter function. To test this hypothesis, the sensitivity of *pic30* mutants to chlorate was assayed. Chlorate (a transport analogue of nitrate) is transported into plants through several nitrate transporters, and wild type Arabidopsis plants are highly susceptible to chlorate-induced leaf bleaching (Bagchi *et al.*, 2012).

Chlorate sensitivity assays were performed at both seedling and adult stages. While no difference was observed among wild type and the three *pic30* mutants under control conditions, pronounced cotyledon and leaf bleaching was observed in wild type, *pic30-1*, and *pic30-2*, but not in *pic30-3* (Figure 7a,b), indicating that *pic30-3* mutant seedlings/plants are insensitive to chlorate-induced necrosis and leaf bleaching.

Complementation of chlorate sensitivity in *PIC30-HA* and *PIC30-OX* lines was also tested at both seedling and adult stages. While *PIC30-HA* seedlings showed wild type sensitivity when grown on chlorate-containing medium (Figure S5a), *PIC30-OX* lines displayed hypersensitivity to chlorate (Figure S5b). Furthermore, 3-week-old adult *PIC30-HA* and *PIC30-OX* plants irrigated with chlorate solution displayed wild type sensitivity to chlorate (Figure 7c,d). These observations confirmed that ectopic expression of wild type *PIC30* can restore chlorate sensitivity in *pic30-3*, presumably by restoring a chlorate transport function.

© 2019 The Authors
The Plant Journal © 2019 John Wiley & Sons Ltd,

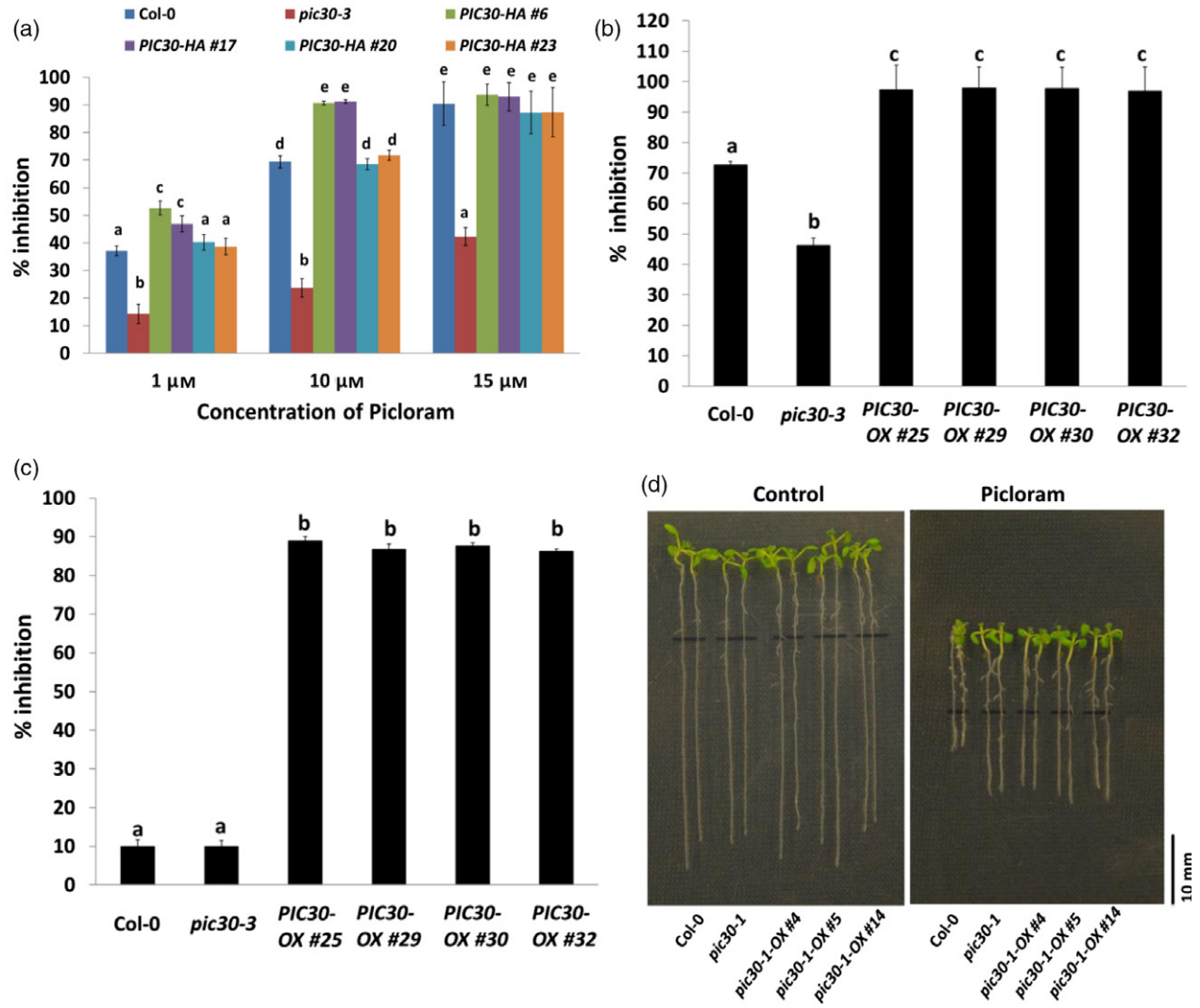

Figure 4. Ectopic expression of *PIC30* complements picloram insensitivity of *pic30-3*.
(a) Primary root growth of *PIC30-HA* lines shows varied sensitivity to picloram. (b, c) Primary root growth of *PIC30-OX* lines is more sensitive than wild type at both 10 µM (b) and 100 nM (c) picloram. (d) Primary root growth of *pic30-1-OX* transgenic lines is insensitive to 10 µM picloram. For root growth assay, 4-day-old seedlings were transferred to ATS (control) medium and ATS medium containing either 100 nM or 10 µM of picloram and root lengths were measured after 4 days of incubation. Black lines on the plates indicate the position of the root tip soon after the transfer of seedlings to treatment plates. Each data point reflects the MPI ($n = 15$), and bars represent SEM. Statistical significance between the samples was determined by one-way ANOVA with Tukey's post-hoc test ($P < 0.01$). Statistical significance is indicated by different letters.

To further test whether disruption of PIC30 affects nitrate uptake, an *in planta* nitrate uptake assay was performed using $^{15}NO_3^-$. Nine-day-old seedlings grown on medium that lacked nitrate were transferred to medium containing 10 mM $K^{15}NO_3$ and the relative uptake of ^{15}N was determined by using a stable isotope mass spectrometer. The results showed that $^{15}NO_3^-$ uptake (as reflected in $\delta^{15}N$) in *pic30-3* is reduced by 40% compared with wild type seedlings (Figure S5c). Moreover, in two of the *pic30-3* complemented lines tested, $^{15}NO_3^-$ uptake was found to be significantly enhanced compared with *pic30-3* (Figure S5c), suggesting that ectopic expression of *PIC30* in *pic30-3* partially restored its nitrate uptake ability.

Expression of *PIC30* is subjected to developmental and diurnal changes

To study the tissue/organ specific expression pattern of *PIC30* gene, we used a combination of qRT-PCR and histochemical GUS staining/fluorometric MUG assay with wild type and transgenic plants carrying the $PIC30_{pro}$*::PIC30-GUS* reporter construct, respectively. Samples were collected from different tissues of mature plants and seedlings, and expression of *PIC30* was examined by qRT-PCR. While *PIC30* transcript was detected at both seedlings and different tissues of mature wild type plants, it was relatively more abundant in rosette leaves (Figure S6a).

© 2019 The Authors

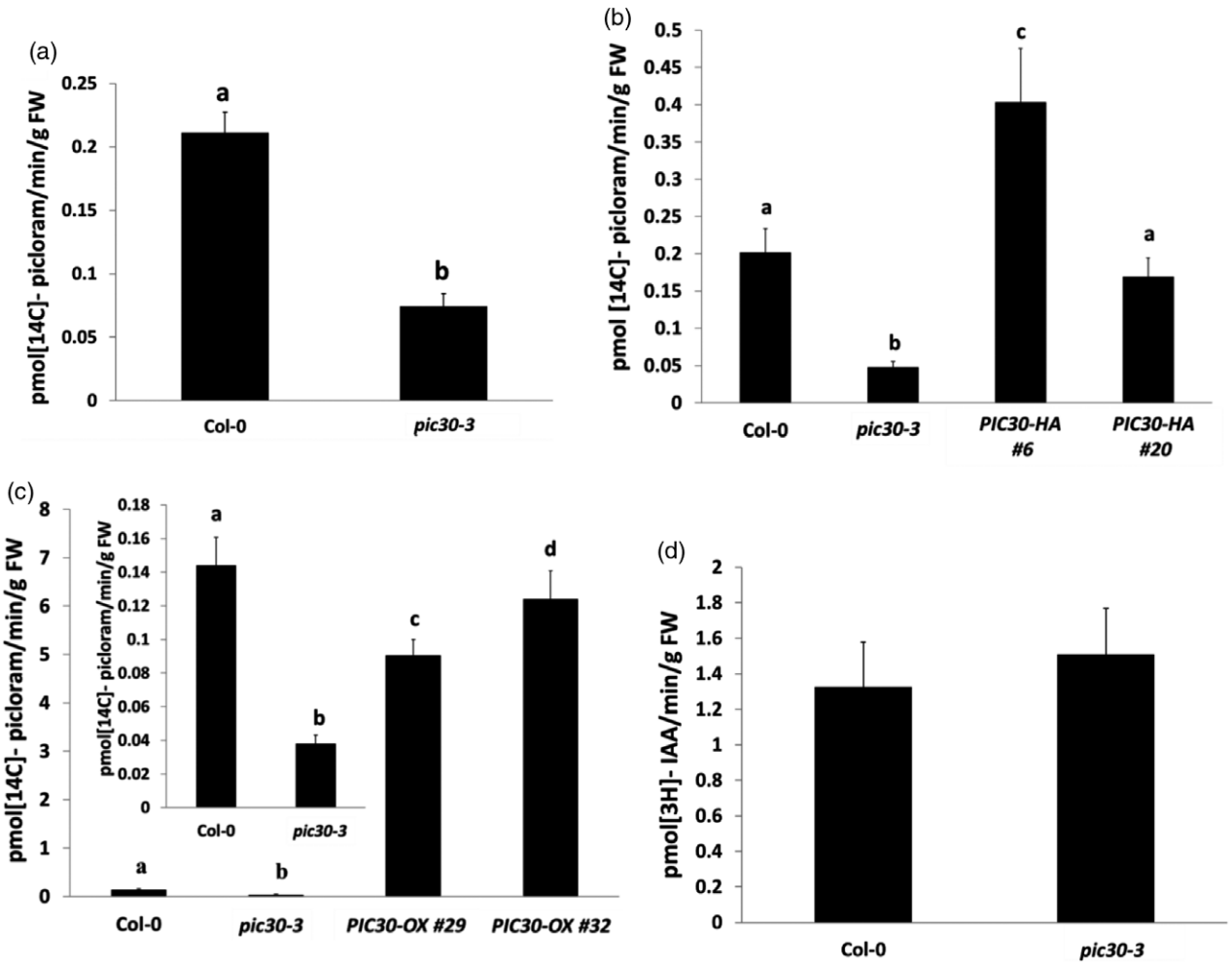

Figure 5. *pic30-3* mutant is defective in picloram uptake.
(a) *pic30-3* mutant is defective in uptake of radiolabelled picloram. (b) Two *PIC30-HA* lines show the different degrees of picloram uptake ability. (c) Picloram uptake is enhanced in *PIC30-OX* transgenic lines. Inset is included to clearly show the uptake difference between wild type and *pic30-3*. (d) Radiolabelled IAA uptake is not defective in *pic30-3*. Fifteen apical root sections (15 mM) were incubated in TAB containing radioactive ^{14}C-picloram or ^{3}H-IAA. After incubation, root sections were rinsed thoroughly using ice-cold TAB buffer and radioactivity was measured using the scintillation counter. Each data point shows mean of three independent replicates, and bar represents SD. Statistical significance between the samples was determined by either Student's *T*-test (a, d) or one-way ANOVA (b, c) with Tukey's post-hoc test ($P < 0.01$). Statistical significance is indicated by different letters.

Histochemical GUS staining also revealed a similar pattern of expression (Figure S6b–g). Interestingly, PIC30 expression was stronger in old rosette leaves than in relatively younger leaves (Figure S6d). Moreover, compared with high level of PIC30 expression in mature flowers, relatively low level of expression was observed in both flower buds and immature flowers (Figure S6e).

At the seedling stage, higher level of *PIC30* expression was observed in 8-day-old seedlings compared with 4-day-old seedlings (Figure S6b,c), suggesting that *PIC30* gene expression may be developmentally regulated. To further study the effect of developmental stage on *PIC30* gene expression, PIC30-GUS activity was tracked from the 1st to 7th day after germination, at 24 h intervals. It was observed that the level of PIC30-GUS expression goes up with the age of the plant, at least within the tested period (Figure S6h).

As *PIC30* was identified in a picloram-based mutant screen, and is likely to function as a nitrate transporter, the effect of picloram and nitrate treatment on *PIC30* expression was tested. The results showed that picloram did not influence the *PIC30* gene expression (Figure S6i). However, nitrate induced the expression of PIC30 in a dose-dependent manner (Figure S6j). The expression of many genes involved in nitrate transport is diurnal. As PIC30 is also permeable to nitrate we speculated that expression of *PIC30* may also be subjected to diurnal variation. To test this possibility, seedlings were grown under a 12 h light/12 h dark regime, and samples were collected at 6-h time intervals. qRT-PCR analysis revealed that the expression of *PIC30*

© 2019 The Authors
The Plant Journal © 2019 John Wiley & Sons Ltd,

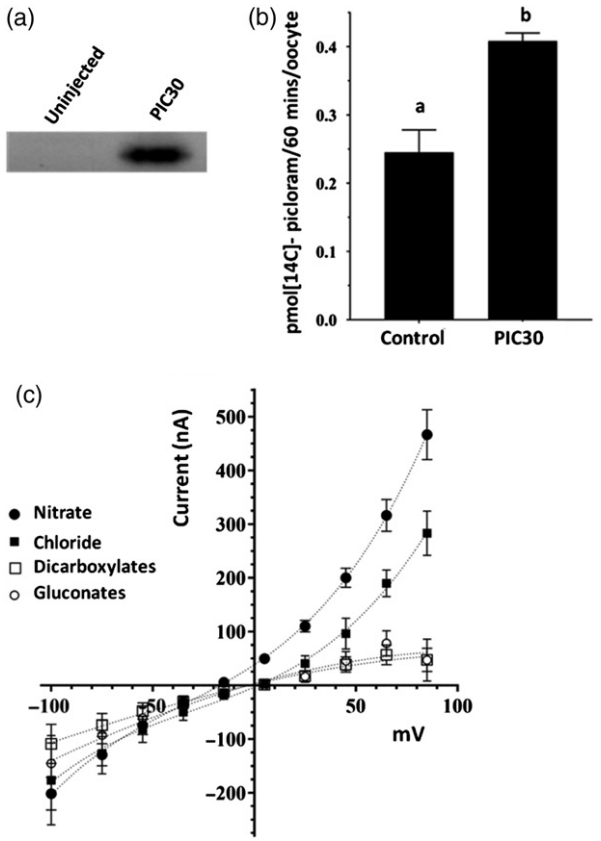

Figure 6. PIC30 transport activity in *Xenopus* oocytes.
X. laevis oocytes were microinjected with 45 ng of cRNA and were assayed for picloram uptake and two-electrode voltage clamp after 3–4 days of culture.
(a) PIC30 cRNA injected and negative control oocytes were homogenized, and protein was separated by SDS-PAGE and transferred to PVDF membrane. Immunoblotting was performed using anti-PIC30 antibody.
(b) *X. laevis* oocytes (control and PIC30-expressing) were assayed for picloram uptake by incubation in medium containing radioactive ^{14}C-picloram, as described in Experimental procedures. Each data point represents the mean, and bars represent SEM (n = 3 for uninjected controls, and n = 5 for PIC30). The experiment was repeated three times with similar results. Statistical significance between the samples was determined using Student's *T*-test. Statistical significance was indicated by different letters.
(c) Current–voltage plots of PIC30 oocytes from two-electrode voltage clamp recording in the presence of 100 mM of the sodium salts of the indicated anions in a base of Ringer's buffer of 5 mM HEPES-NaOH, 6 mM $CaCl_2$, 5 mM $MgCl_2$, 2 mM KCl. The PIC30 currents were standardized by background correction of currents observed with negative control uninjected oocytes with the same buffer formulations. The values represent the average currents (n = 3 oocytes) with the error bars showing the SEM.

was diurnally regulated with the highest expression at the dawn (Figure S6k).

DISCUSSION

PIC30 contains putative MFS- and NOD- domains and localizes to the plasma membrane

Despite some similarities in plant responses to various auxinic chemicals, many differences in response have also been reported. While IAA, 2,4-D and 1-NAA interact with the same auxin co-receptors, TIR1, AFB1, AFB2 and AFB3, picloram interacts with AFB4 and AFB5 (Prigge *et al.*, 2016), suggesting that the mode of action of picloram may be considerably different from other commonly used auxinic chemicals. Even with functional similarities, differences exist in transport of different auxinic chemicals (Ito and Gray, 2006; Ruzicka *et al.*, 2010). Despite its use as a commercial herbicide for long, proteins involved in picloram transport into plant cells have not been found so far. As picloram is a synthetic chemical, it should be transported as a secondary substrate via a native transporter protein. Our results indicate that Arabidopsis *PIC30*, which has been mapped to the *At2g39210* locus, encodes a transporter protein that contains a MFS- and a NOD- domain. We identified three allelic mutants of *PIC30* (*pic30-1*, *pic30-2*, and *pic30-3*) containing point mutations in this locus (Figure 1a). The following three experimental evidences indicated that the mutation in *pic30* is responsible for the picloram related phenotypes: (1) All three are semidominant mutants (Figure 1d) and confer picloram insensitivity (Figure 1b,c); (2) Overexpression of *pic30-1* confers picloram insensitivity in wild type (Figure 4d); and (3) Ectopic expression of *PIC30* in *pic30-3* confers picloram sensitivity (Figure 4a,b). As *PIC30* transcript in *pic30-3* contains premature in-frame stop codons (Figure S1c,d), it may produce a highly truncated protein if translated. Therefore, the *pic30-3* mutant was selected as an alternative for a knockout mutant in our studies. The three mutant alleles showed both similar and variable phenotypes due to the positioning of point mutations, allowing us to draw valuable information about the possible involvement of different domains in PIC30 function.

Several MFS proteins have been previously characterized and, most importantly, many of the proteins identified in this family so far have been implicated as membrane localized transporter proteins (Pao *et al.*, 1998; Remy *et al.*, 2013). Co-localization of PIC30–GFP with two plasma membrane markers (Figures 3 and S3) confirms that PIC30 is indeed localized to the plasma membrane, strongly supporting a putative transporter function.

pic30 mutation causes selective insensitivity against picolinate herbicides

Previous studies have characterized several picolinate insensitive signalling mutants (Walsh *et al.*, 2006; Prigge *et al.*, 2016). Walsh *et al.* (2006) identified several recessive mutant alleles of *SGT1* and *AFB5*, which were specifically insensitive to picolinate herbicides. In a later study using *in vitro* pull-down assays, Prigge *et al.* (2016) suggested that AFB4 and AFB5 F-box proteins are the targets of picolinate herbicides. In contrast, *pic30* mutants show a semidominant trait (Figure 1d). This observation along with the selective insensitivity to picolinate herbicides

© 2019 The Authors

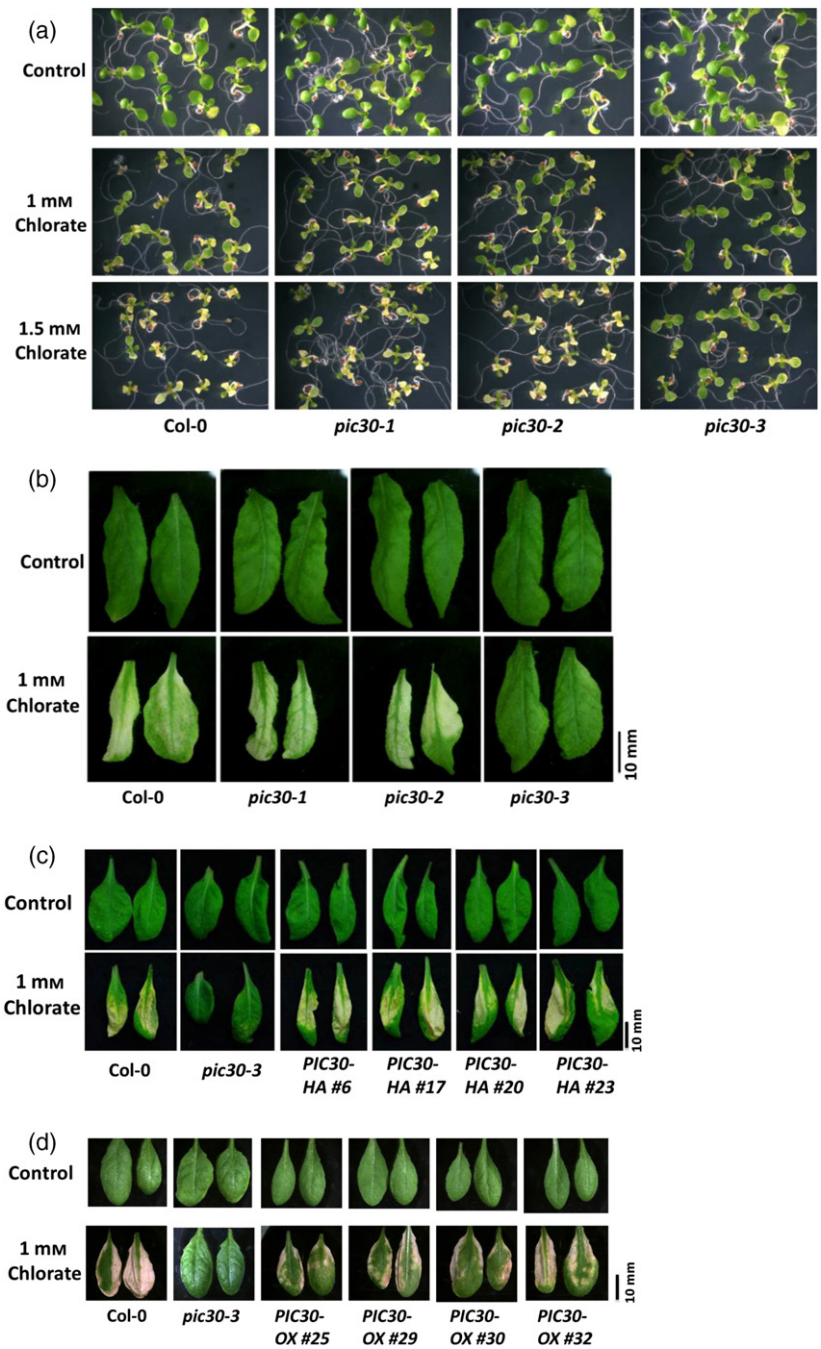

Figure 7. *pic30-3* is insensitive to chlorate ions.
(a, b) *pic30-3* but not *pic30-1* or *pic30-2* mutant seedlings or plants are insensitive to chlorate-induced necrosis and beaching. (c) *PIC30-HA* and (d) *PIC30-OX* complement chlorate sensitivity in *pic30-3*.
For chlorate sensitivity assay during the seedling stage, seeds were plated either on ATS (control) or ATS containing the indicated concentration of sodium chlorate and incubated for 9 days. For chlorate sensitivity test during the adult stage *c.* 3-week-old plants were irrigated with 1 mM sodium chlorate on every alternative day. Images were acquired 12 days after the first sodium chlorate treatment. Experiments were repeated three times with similar results.

(Figure 2a–f), and plasma membrane localization of PIC30 (Figure 3), collectively led us to the initial speculation that the PIC30 protein may be specifically involved in picloram transport rather than in signalling cascade. As mutations in *PIC30* resulted in picloram insensitivity, and the heterozygote conferred partial insensitivity to picloram, it is logical to assume that the PIC30 protein may function in picloram influx. As the members of the MFS family are often implicated as general transporters in plants (Remy *et al.*, 2013), we hypothesized that PIC30 may be involved in the transport of picloram and some natural compounds, analogous to Arabidopsis PDR9 protein, a member of the ABC transporter family, which transports both 2,4-D and IBA (Ito and Gray, 2006; Ruzicka *et al.*, 2010).

PIC30 transports picloram into the cells

Many proteins containing MFS domains are known to transport solutes, amino acids, hormones and nutrients (Remy *et al.*, 2013; Denance *et al.*, 2014). Therefore, we investigated the possible transporter function(s) of PIC30,

© 2019 The Authors
The Plant Journal © 2019 John Wiley & Sons Ltd,

focusing on its ability to transport picloram and other naturally occurring substrates. All three *pic30* mutants showed specific insensitivity to the picolinate herbicides, picloram and aminopyralid, but demonstrated wild type sensitivity to the other commonly used synthetic auxins, 2,4-D and 1-NAA as well as the natural auxin IAA (Figure 2a–f). This observation is further supported by picloram hypersensitivity (Figure 4b,c) and wild type IAA or 1-NAA sensitivity (Figure S4e,f) of the lines that overexpressed *PIC30* on a *pic30-3* background. Collectively, these data indicated that PIC30 is involved in transport of picolinate herbicides. Using radiolabelled ^{14}C-picloram, we have confirmed that *pic30-3* (Figure 5a), as well as *pic30-1* and *pic30-2* (Figure S4h), is defective in the uptake of picloram compared with wild type. This observation along with the semidominant nature of the mutation, localization of PIC30 protein to the plasma membrane and the presence of an MFS domain strongly supported the notion that PIC30 is involved in picloram influx. Alternatively, PIC30 may be regulating another transporter protein thereby indirectly influencing picloram transport. However, this is highly unlikely, because when the same radioactive picloram transport assay was performed using transgenic lines that overexpress *PIC30* gene in *pic30-3* background (Figure 5c), or heterologous expression of PIC30 in *X. laevis* oocytes (Figure 6a,b) resulted in significantly higher accumulation of picloram, indicating that PIC30 is indeed an influx transporter of picloram.

pic30 mutant transcript level is affected by NMD pathway

As described above, the transcript level of *PIC30* is significantly lower in all three mutants compared with that of wild type (Figure S2a,b). This appears to be due to the degradation of mutant transcripts through NMD machinery that predominantly destroys aberrant transcripts with premature stop codons (Chang *et al.*, 2007; Kurihara *et al.*, 2009). Consistent with this, *PIC30* transcript abundance was significantly higher on the NMD mutant *upf3-1* background than on the *pic30-3* mutant background (Figure S2c).

Among the three *pic30* mutants, the steady-state level of the *PIC30* transcript is lowest in *pic30-3* compared with either *pic30-1* or *pic30-2*. Possible reasons for this phenomenon may be the nature and location of the mutation, as well as splicing status of the transcripts. Unlike in either *pic30-1* or *pic30-2*, the transcript of *pic30-3* did not undergo splicing to remove the intron (Figure S1c), resulting in the introduction of premature in-frame stop codons (Figure S1d). Similar to *pic30-3*, the mutation in *pic30-2* also resulted in a premature stop codon, but closer to the 3 end of the transcript; therefore the transcript may be less vulnerable to the NMD pathway. Consistent with this, the *pic30-1* mutant transcript is least subjected to mRNA degradation as it has a missense mutation that does not introduce a premature stop codon. Taken together, our results clearly showed that the NMD pathway affected *pic30* transcript abundance in Arabidopsis, which should be taken into consideration during future manipulations of this gene.

Diurnal variation of PIC30 expression and its function in anion transport in Arabidopsis

While genetic and biochemical data provided strong evidence for a role of PIC30 in picloram uptake, the identity of endogenous substrate for this transporter remains questionable. PIC30 is part of a MFS superfamily that contains the conserved nodulin-like (NOD) and MFS domain (pfam 06813) that are characteristic of the soybean and *Lotus japonicus* nodulin 70 transporters (Vincill *et al.*, 2005). Similar to these proteins, PIC30 showed permeability to anions, with a preference for inorganic anions including nitrate and chloride. In nodules, these proteins are found on the symbiosome membrane that houses endosymbiotic nitrogen fixing rhizobia. While GmN70 and LjN70 do not show apparent H^+ or cation-coupled transport activities, they are proposed to be coupled indirectly to proton gradients through a proton pumping ATPase found on the symbiosome membrane (Vincill *et al.*, 2005). Experimental evidence suggested that an endogenous function of PIC30 may be the transport of anions, including nitrate as discussed below. However, whether this transport function of PIC30 is directly coupled to other ions or indirectly to a proton gradient is not clear at this time.

Nitrate transporter proteins from different plant species have also been implicated in chlorate transport, rendering plants sensitive to exogenous applications of chlorate (Bagchi *et al.*, 2012). Mutants that are defective in nitrate influx showed insensitivity to chlorate-induced cotyledon and leaf bleaching, providing a simple, yet powerful, screening tool to test mutants impaired in nitrate transport (Bagchi *et al.*, 2012). *In planta* chlorate sensitivity assays showed chlorate insensitive phenotypes in *pic30-3* (Figure 7a,b), while the overexpression of *PIC30* on the *pic30-3* background restored the sensitivity to chlorate (Figure 7c,d), implying that PIC30 may function in nitrate uptake in Arabidopsis. However, both *pic30-1* and *pic30-2* mutations did not affect the chlorate sensitivity phenotype. Several factors could explain the more severe phenotype exhibited by *pic30-3*. Most importantly, this mutant results in intron retention that leads to: (1) The induction of a strong NMD response that strongly suppresses the abundance of *pic30-3* transcript (Figure S2a,b); and (2) Due to early premature stop codon, *pic30-3* may result in a severely truncated (~20% of full length) and dysfunctional protein product. In contrast, *pic30-1* and *pic30-2* showed higher expression of transcripts compared with *pic30-3* and would produce larger proteins with either a single mutation within the NOD domain (*pic30-1*) or a stop codon that would produce a

© 2019 The Authors

shortened protein with the complete NOD domain and a partial MFS domain (*pic30-2*). While all three mutants showed defects in picloram uptake (Figure S4h), it is possible that mutated proteins in *pic30-1* and *pic30-2* are still capable of functionally transporting chlorate into the plant at concentrations that are inhibitory.

To directly assay nitrate uptake in the most severe mutant (*pic30-3*), $^{15}NO_3^-$ uptake experiments were performed with wild type and *pic30-3* plants. $^{15}NO_3^-$ uptake is reduced by 40% in *pic30-3* seedlings compared with wild type, and is partially restored in *pic30-3* complemented lines (Figure S5c). Taken together, the *Xenopus* oocyte data, chlorate sensitivity analysis, and $^{15}NO_3^-$ uptake analysis supported a potential contribution of *PIC30* in the uptake of nitrate in Arabidopsis.

The *PIC30-OX* lines showed hypersensitivity to chlorate during the seedling stage (Figure S5b), but showed wild type sensitivity at the adult stage (Figure 7d). The same overexpression lines are hypersensitive to picloram at both seedling (Figure 4b) and adult stages (Figure S4d). The explanation for this difference in chlorate and picloram sensitivities is unclear, however it is likely that transport of chlorate/nitrate may be tightly regulated to bring in an optimum level of nitrate into the plant system, while no such mechanism prevails for picloram transport.

While it is not restricted to nitrate transporters, diurnal variation in gene expression is a characteristic of many genes that are involved in either nitrate transport or metabolism. The expression of several genes involved in nitrate transport is elevated during day-time to transport nitrate into the plant system and its subsequent loading into the appropriate tissues/organs (Lin *et al.*, 2008; Fan *et al.*, 2009; Li *et al.*, 2010). Expression of the *PIC30* gene is also regulated diurnally, with a relatively higher expression during day-time than at night-time (Figure S6k). Moreover, *PIC30* strongly expresses in roots during both cotyledon and adult stages, implying that PIC30 might be involved in uploading nitrate (and other possible inorganic anions) into the roots during day-time. It is not uncommon that endogenous nitrate transporters also transport other molecules. A more recent study indicated that the NRT1/PTR family (NPF) proteins that transport nitrate or di-/tri-peptides also transport various plant hormones (Chiba *et al.*, 2015). While we do not know whether PIC30 is involved in the transport of endogenous plant hormones, the data presented here clearly show that it is involved in transporting synthetic auxin, picloram, and electrophysiological data indicated that it is permeable to anions with a preference for nitrate.

In summary, findings in the present study involving *in planta* chlorate transports assays, and anion transport assays in *Xenopus* oocytes using heterologous expression of PIC30, strongly suggested that PIC30 functions as a nitrate and/or anion transporter, which also transports picloram as a secondary substrate. The mechanism of PIC30 transport, including the potential roles of proton coupling, as well as its role in ion homeostasis and how it might coordinate transport of nitrate or other physiological anions in *planta*, remains a subject for future study.

Potential implications of *PIC30* gene in agriculture

Putative *PIC30* orthologues are present in several commercially important crop plants, including soybean and maize (Vincill *et al.*, 2005; http://caps.ncbs.res.in/stifdb2/index.html) and in forest species. Therefore, present knowledge on the role of PIC30 in picloram/nitrate transport and the impact of different point mutations on PIC30 functions could be used for the possible genetic manipulation of commercially and environmentally important plants species. Considering the facts that mutation in *pic30-1* abolishes picloram transport function without disrupting its nitrate transport ability, and that overexpression of *pic30-1* in wild type confers an insensitivity to picloram, may be used in genetic manipulation of picloram sensitivity in plants without altering the transport of nitrate. While some picolinate herbicides have a relatively longer half-life in soil (Johnsen, 1980; Smith *et al.*, 1988) and are not suitable for use in farmlands, 6-aryl-picolinates that have been discovered recently can be used for cereal crops (Epp *et al.*, 2016). If 6-aryl-picolinates use the same transporter system as picloram, it would be possible to exploit this transporter system to generate picolinate-resistant dicot crops.

Additionally, a few weeds have already developed resistance to picloram (Busi *et al.*, 2017). While the exact genetic basis of resistance in these weeds is not yet known, it is possible that picloram resistance of at least some of these weeds may be due to defects in picloram uptake and transport, as the case in *pic30* mutants. The better understanding of the genetic basis of picloram resistance will also help to improve weed management practices.

EXPERIMENTAL PROCEDURES

Plant material and growth conditions

Wild type and mutant Arabidopsis seeds used in this study were on the Col-0 background. Seeds were surface sterilized with 2.4% sodium hypochlorite solution containing 0.01% Triton X-100, then rinsed thoroughly with sterile distilled water before plating onto the nutrient medium. Unless specified, *Arabidopsis thaliana* nutrient medium with 1% sucrose (ATS; Lincoln *et al.*, 1990) was used.

To study the diurnal variation of *PIC30* gene expression, Col-0 seeds were plated on medium and incubated at 21°C under 12 h light/12 h dark cycles. Starting from the 7th day, seedling samples were collected at 6-h time intervals for indicated durations and frozen in liquid nitrogen. cDNA was prepared from total RNA extracted from the seedlings, and qRT-PCR was performed.

© 2019 The Authors
The Plant Journal © 2019 John Wiley & Sons Ltd,

To study the effect of picloram on *PIC30* expression, 5-day-old *PIC30*$_{pro}$::*PIC30-GUS* seedlings were treated with 25 μM picloram in liquid medium by incubating under continuous light at 21°C without shaking. Samples were collected at different time intervals and frozen in liquid nitrogen. PIC30-GUS expression was determined through quantitative MUG assay (Parry *et al.*, 2006).

For root growth inhibition assays, 4- to 5-day-old seedlings were transferred to control ATS medium and ATS containing the indicated concentrations of different auxins. Primary root length was measured after 4 days of incubation, and percentage root growth inhibition was calculated.

To test auxin-induced *DR5::GFP* expression, 5-day-old seedlings were transferred to control ATS, and ATS containing indicated concentrations of different auxins. Plates were incubated for 20 h at 21°C under continuous light. Confocal images were acquired after the incubation period.

Isolation, identification, and positional cloning of *pic30* mutants

Approximately 70 000 Arabidopsis (Col-0) seeds were mutagenized with EMS as previously described (Kim *et al.*, 2006). M1 seeds were germinated on soil and grew under continuous light at 22°C. M2 seeds were collected and bulked from these plants and screened on ATS medium containing 10 μM picloram. Seedlings that showed insensitivity in primary root growth to picloram were selected. These mutants were back-crossed to wild type Col-0 four times to remove any secondary mutations. Homozygous mutants were then crossed with wild type, Landsberg *erecta* (L*er*) for generating mapping populations.

The *pic30* alleles were located to the bottom arm of chromosome 2 using InDel and single nucleotide polymorphism (SNP) mapping primers suggested by the Monsanto L*er* polymorphism collection available through The Arabidopsis Information Resource (TAIR) website. All three alleles were fine mapped to a region of 73 kb within the annotation unit T16B24, between gene loci *At2g39110* and *At2g39260*. Sequencing of candidate genes within this region identified the mutations in *At2g39210* gene in all three allelic mutants.

Preparation of gene constructs and plant transformation

To prepare *PIC30*$_{pro}$::*PIC30-GUS* transgenic lines, full-length *PIC30* gene and a 2.4 kb region upstream of the ATG was amplified from wild type genomic DNA using the primers PIC30-PROMXho1-F and PIC30BamH1-R (Table S1) and phusion DNA polymerase (NEB). The PCR product was cloned into the pBluescript SK cloning vector, and then subcloned into the pBI101.1 vector carrying the GUS reporter gene at the COOH terminus. The recombinant vector was shuttled into *Agrobacterium* strain GV3101 and transformed into wild type plants using floral dip method (Clough and Bent, 1998).

To prepare CaMV *35S*$_{pro}$::*pic30-1-myc* (*pic30-1-OX*) transgenic lines, full-length *PIC30* coding region without the stop codon was amplified from CD4-31 cDNA library, using primers PIC30*Bam*H1-F and PIC30*Xho*I-R (Table S1) and phusion DNA polymerase (NEB). The PCR product was then cloned into pBluescript SK vector, and *pic30-1* mutation was introduced by site directed mutagenesis using primers, PIC30-mutF and PIC30-mutR (Table S1). The *pic30-1* fragment was released by digesting with *Bam*HI and *Xho*I, and subcloned into *Bam*HI and *Sal*I sites of a modified pROKII vector carrying a 5.5X *myc* epitope in-frame. The recombinant vector was shuttled into the *Agrobacterium* strain GV3101 and transformed into wild type plants.

To prepare *CaMV 35S*$_{pro}$::*PIC30-GFP* (*PIC30-OX*) transgenic lines, the full-length *PIC30* gene including the intron was amplified without the stop codon, using PIC30*Bam*H1-F and PIC30*Xho*I-R primers (above). It was directionally cloned into pENTR/D-TOPO vector (Invitrogen, Carlsbad, CA, USA) and transferred into pB7WG2.0 Gateway vector using the LR clonase kit, according to manufacturer's instructions (Invitrogen). The recombinant pB7WG2.0 vector containing *PIC30* gene was shuttled into *Agrobacterium* strain GV3101, and transgenic plants expressing *PIC30*-GFP were generated in *pic30-3* mutant background.

To prepare *PIC30*$_{Pro}$::*PIC30-HA* (*PIC30-HA*) transgenic lines, a 2.4 kb promoter plus coding sequence was amplified using primers PIC30PROMXhoI-F and PIC30BamHI-R (Table S1). It was directionally cloned into the *pENTR/D-TOPO* vector (Invitrogen) and transferred into *pEarleyGate301* Gateway vector using the LR clonase kit, according to manufacturer's instructions (Invitrogen, USA). The recombinant *pEarleyGate301* vector was shuttled into *Agrobacterium* strain GV3101, and transgenic plants expressing *PIC30-HA* were generated in *pic30-3* mutant background.

To prepare PM-RK/*35S*$_{pro}$::*PIC30-GFP* lines, PM-RK (CD3-1007, Nelson *et al.*, 2007) was obtained from Arabidopsis Resource center (ABRC, Columbus, OH, USA, Ohio State University). PM-RK was shuttled into *Agrobacterium* strain GV3101 and transformed into transgenic plants carrying *35S*$_{pro}$::*PIC30-GFP*.

RNA extraction and qRT-PCR analysis

For qRT-PCR analysis, wild type, mutant or transgenic seedlings were immediately frozen in liquid nitrogen following treatment conditions. Total RNA was extracted using TRI Reagent (Sigma, St. Louis, MO, USA) and the contaminating DNA was removed using RNase-free DNase treatment. cDNA was synthesized from 1 μg of total RNA using Superscript reverse transcriptase following the manufacturer's instructions (Invitrogen). Primer sequences used in qRT-PCR are listed in Table S1. Setting-up the qRT-PCR and primer efficiency was described elsewhere (Jayaweera *et al.*, 2014). Ubiquitin-associated (UBA, *At1g04850*) housekeeping gene was used as the internal control throughout the qRT-PCR analyses and relative expression level was calculated using the comparative C_T method, while the $2^{-\Delta\Delta C}{}_T$ value of the control samples was normalized to 1.

Qualitative and quantitative GUS expression analysis

For histochemical GUS staining, seedlings or tissues were fixed and stained as described previously (Parry *et al.*, 2006). After staining, seedlings/tissues were transferred to 70% ethanol to remove chlorophyll, then imaged using a Nikon SMZ 1500 stereomicroscope.

Quantification of GUS expression was performed by fluorometric MUG (4-methylumbelliferyl--D-glucuronide) assay following the protocol described elsewhere (Parry *et al.*, 2006) and the fluorescence was measured using a fluorometer (Modulus, Turner Biosystems).

Confocal imaging

Confocal images were acquired using either a ×20 water immersion or a ×60 oil immersion lenses with Fluoview FV1000 laser scanning confocal microscope (Olympus, Center Valley, PA, USA). When making a quantitative comparison between two or more confocal images, similar laser intensity and transmittance light were used.

© 2019 The Authors

In planta chlorate and picloram sensitivity test

For chlorate sensitivity testing at the seedling stage, seeds were plated onto either control medium or medium containing 1 mM or 1.5 mM sodium chlorate. Plates were incubated under continuous light at 21°C for 9 days. After the incubation, representative images were acquired using a digital single lens reflex (DSLR; Pentex) camera.

For chlorate and picloram sensitivity testing at the adult stage, 7-day-old seedlings were transferred to soil (Fafard growing mix 2) and grown under continuous light for an additional 12 days. To test chlorate sensitivity, plants were then irrigated with 1 mM sodium chlorate solution on alternate days. Chlorate-induced leaf bleaching were examined and imaged after 10–12 days. To test picloram sensitivity, plants were sprayed with 100 or 200 g/ha of picloram as described in Walsh *et al.* (2006). Images were acquired 14–18 days after treatment.

SDS-PAGE and immunoblotting

Total plant protein was extracted from 7-day-old seedlings in denaturation extraction buffer (125 mM Tris–HCl pH 8.8, 1% SDS, 10% glycerol, 50 mM $Na_2S_2O_5$), and the protein concentration was determined using Bradford's method. Total protein was separated using 10% sodium dodecyl sulfate polyacrylamide gel electrophoresis (SDS-PAGE) and transferred to polyvinylidene difluoride (PVDF; Bio-Rad, Hercules, CA, USA) membrane. Immunoblotting was performed using either anti-GFP (Santa Cruz Biotechnology, Dallas, TX, USA) or anti-Myc (Covance, Princeton, NJ, USA) primary antibody, followed by appropriate secondary antibody. Bands were observed using the Enhanced Chemiluminescence 2 kit (Pierce, Waltham, MA, USA) as per manufacturer's instructions.

In planta radioactive transport assay

In planta transport assays were performed according to the protocol described elsewhere (Ito and Gray, 2006) with few modifications. Here, 15 mM root sections (at root tip) from 15 9-day-old seedlings were excised and incubated in transport assay buffer (TAB; 20 mM MES-KOH, pH 5.6, 10 mM sucrose and 0.5 mM $CaCl_2$) for 30 min. Root sections were then transferred to TAB containing 1.5 nM of ^{14}C picloram and 10 μM unlabelled picloram or 7.9 nM of ^{3}H IAA and 100 nM unlabelled IAA, and incubated for 6 h at room temperature. After rinsing with cold TAB buffer, root sections were transferred to scintillation vials containing 1 ml of scintillation liquid. Radioactivity was measured using an LS6500 scintillation counter (Beckman Coulter, CA).

Construction of oocyte expression vector and analysis of PIC30 transport function in oocytes

PIC30 ORF was cloned into the *Bgl*II and *Spe*I sites of the modified *Xenopus* expression vector pT7TS-Flag (Krieg and Melton, 1984) carrying the M2 Flag epitope DNA sequence in-frame with a final codon from *PIC30*. Capped cRNA was synthesized by an *in vitro* transcription using the mMESSAGE mMACHINE™ kit (Ambion, Austin, TX, USA) as described earlier (Vincill *et al.*, 2005). *Xenopus laevis* oocytes (of stages V and VI) were surgically harvested and microinjected with 45 ng of cRNA. Microinjected and uninjected control oocytes were cultured in Frog Ringer's solution (Vincill *et al.*, 2005) supplemented with 1000 U/ml penicillin–streptomycin at 18°C for 3–4 days before analysis. GmN70 expression in oocytes was carried out as previously described (Vincill *et al.*, 2005).

Oocyte recordings were done by two-electrode voltage clamp using an Oocyte Clamp Amplifier model OC-725C (Warner Instruments, Hamden, CT, USA). The microelectrodes were filled with 3 M KCl and tipped with 2% agarose-3 M KCl to reduce KCl leakage (electrode resistances <1.5 MΩ). The Warner OC-725C instrument is equipped with a virtual ground bath headstage containing a sense electrode (positioned close to the oocyte) and a bath electrode, which are configured to clamp the bath potential to zero, eliminating the need for series resistance compensation. The standard recording bath solution consisted of 2 mM KCl, 5 mM $MgCl_2$, 6 mM $CaCl_2$, 5 mM HEPES-NaOH, pH 7.6 containing 100 mM of the sodium salt of the test anion conductant (chloride, nitrate, gluconate or dicarboxylate, final solution osmolarity = 215 mOsm/kg). For dicarboxylates, an equal molar mixture of sodium succinate and sodium malate was used as described previously (Vincill *et al.*, 2005).

Recordings were performed using a stepwise voltage protocol, in which the oocyte Vm was clamped from +80 to −160 mV in 20 mV increments, and currents were recorded for 1 sec increments at each applied voltage. Voltage pulses were controlled with the Labscribe program suite version 1.6 (iWork/CB Sciences Inc, NH, USA). Membrane current (Im) output was filtered at 1 kHz with a four-pole Bessel Filter, was digitized via the iWork/118 analogue to digital converter hardware, and was analyzed using Labscribe software. Reversal potentials were determined from I–V plots with the current readings values obtained at 1 sec after the applied voltage was administered. PIC30 permeability comparisons for the various anions were carried out by substitution of background currents obtained with negative control oocytes (uninjected or injected with an equivalent volume, 46 nl, of sterile water) under identical conditions.

^{14}C-Picloram uptake was carried out as follows. Four days after injection with *PIC30* cRNA or sterile water, oocytes in batches of three were pre-incubated in 5 mM MES-NaOH (pH 5.5), 6 mM $CaCl_2$, 5 mM $MgCl_2$, and 96 mM NaCl at room temperature for 30 min. The oocytes were then placed into the assay medium, which contained the same buffer containing 10 mM ^{14}C-picloram (5 μC_i/ml). Uptake was carried out at room temperature (22°C) for 30 min, oocytes were washed with an excess (15 ml) of ice-cold buffer without picloram, oocytes were lysed in 10% SDS, and were counted for ^{14}C by scintillation counting.

In planta $^{15}NO_3^-$ transport assay

Surface-sterilized seeds of Arabidopsis wild type Col-0, *pic30-3*, and two *pic30-3* complementation lines of $PIC30_{Pro}$*::PIC30-HA* were grown on nitrate-free medium with ammonium succinate as the sole nitrogen source, as previously described (Wang *et al.*, 2003). Seedlings were grown for 9 days on vertically oriented plates under continuous light at 22°C in a growth chamber. Transport of $^{15}NO_3^-$ into seedlings was assayed as previously described (Remans *et al.*, 2006). Approximately 30 seedlings per treatment were washed in 0.1 mM CaSO4, transferred into nitrate-free liquid medium supplemented with 10 mM $K^{15}NO_3$ (atom % ^{15}N, 99%) for 10 min and washed in 0.1 mM $CaSO_4$. The seedlings were blot dried, placed in a 70°C oven for 2 days and weighed. Dried seedlings were ground to a powder using a mortar and pestle.

Bulk $\delta^{15}N$ values of ground plant material were measured using a Costech elemental analyzer (EA) coupled with a Delta Plus XL Isotope Ratio Mass Spectrometer in the Stable Isotope Laboratory in the Department of Earth and Planetary Science at the University of Tennessee, Knoxville, USA (Sanchez *et al.*, 2017). For $\delta^{15}N$ analyses, dried plant material was packed into tin cups to allow

© 2019 The Authors

complete combustion of the sample inside the EA. δ15N was calculated using the following equation with air–N_2 used as a nitrogen standard. The analytical precision values (standard deviation) for bulk wt %N and $\delta^{15}N$ were 0.3% and 0.9‰ respectively:

$$\delta^{15}\mathrm{N}\frac{\left(\frac{^{15}\mathrm{N}}{^{14}\mathrm{N}}\right)_{\text{sample}}-\left(\frac{^{15}\mathrm{N}}{^{14}\mathrm{N}}\right)_{\text{standard}}}{\left(\frac{^{15}\mathrm{N}}{^{14}\mathrm{N}}\right)_{\text{standard}}}\times 1000\,[‰]$$

Statistical analysis

For root growth assays, mean percentage inhibition (MPI) was calculated using following formula:

$$\mathrm{MPI} = \mathrm{Mean}\left[\begin{array}{c}(\text{Root length on control} - \text{Root length on Treatment})\\ /\text{Root length on control}\end{array}\right]\times 100.$$

Standard deviation was converted to percentage standard error and represented in the graphs throughout.

Student's *T*-test was used to compare the statistical significance between two samples, while analysis of variance (ANOVA) was used to calculate the statistical significance, if more than two samples were present.

ACCESSION NUMBERS

PIC30 (*At2g39210*), UBA (*At1g04850*)

ACKNOWLEDGEMENTS

This research was supported by National Science Foundation CAREER Grant IOS 0845305 (to ND), Research Enhancement Grant from Texas State University (to ND and SD), One-time Grant 90000525 from Texas State University (to ND), and National Science Foundation Grant MCB-1121465 (to DMR). Confocal facility was supported by National Science Foundation grant DBI-0821252 (to J.R. Koke and Dana García, Texas State University, USA). Authors wish to thank Enamul Huq (The University of Texas at Austin) for allowing us to use laboratory equipment and anti-GFP antibody for GFP–western blotting, and Timothy Cioffi for critical reading of the manuscript. Authors greatly appreciate the help of Anna Szynkiewicz and Anthony Faiia in the Department of Earth and Planetary Sciences at University of Tennessee, Knoxville for ^{15}N uptake assay. Authors declare that there is no conflict of interest.

AUTHOR CONTRIBUTIONS

PKK designed and performed mutant characterizations and transgenic experiments, analyzed data, and co-wrote the manuscript; SD designed and performed experiments, mutant isolations and characterizations, analyzed data, and co-wrote the manuscript; EV designed, performed and analyzed data for nitrate transport experiments in frog oocytes; EV and PR designed, performed, and analyzed data for two-electrode voltage clamp experiments in frog oocytes; PR carried out the ^{14}C- uptake experiments in oocytes; IA performed *pic30-3* complementation assays; DR supervised the design of voltage clamp and picloram uptake experiments in *Xenopus* oocytes and co-wrote the manuscript. ND designed the experiments and co-wrote the manuscript.

SUPPORTING INFORMATION

Additional Supporting Information may be found in the online version of this article.

Figure S1. PIC30 phylogeny, predicted topology, and *pic30* mutant positioning.

Figure S2. *pic30* mutant transcript is a target of NMD-mediated RNA degradation pathway.

Figure S3. PIC30-GFP co-localizes with plasma membrane marker PM-RK.

Figure S4. Wild type *PIC30* complements picloram sensitivity in *pic30-3.*

Figure S5. Ectopic expression of *PIC30* complements chlorate insensitivity and defective nitrate uptake of *pic30-3.*

Figure S6. *PIC30* expression is developmentally regulated.

Table S1. Primer sequences that were used in this study.

REFERENCES

Bagchi, R., Salehin, M., Adeyemo, O.S., Salazar, C., Shulaev, V., Sherrier, D.J. and Dickstein, R. (2012) Functional assessment of the Medicago truncatula NIP/LATD protein demonstrates that it is a high-affinity nitrate transporter. *Plant Physiol.* **160**, 906–916.

Busi, R., Goggin, D.E., Heap, I. *et al.* (2017) Weed resistance to synthetic auxin herbicide. *Pest. Manag. Sci.* **74**, 2265–2276.

Büttner, M. (2007) The monosaccharide transporter (-like) gene family in Arabidopsis. *FEBS Lett.* **581**, 2318–2324.

Calderon-Villalobos, L.I., Lee, S., De Oliveira, C. *et al.* (2012) A combinatorial TIR1/AFB-Aux/IAA co-receptor system for differential sensing of auxin. *Nat. Chem. Biol.* **8**, 477–485.

Chang, Y.F., Imam, J.S. and Wilkinson, M.F. (2007) The nonsense-mediated decay RNA surveillance pathway. *Annu. Rev. Biochem.* **76**, 51–74.

Chiba, Y., Shimizu, T., Miyakawa, S., Kanno, Y., Koshiba, T., Kamiya, Y. and Seo, M. (2015) Identification of Arabidopsis thaliana NRT1/PTR FAMILY (NPF) proteins capable of transporting plant hormones. *J. Plant Res.* **128**, 679–686.

Clough, S.J. and Bent, A.F. (1998) Floral dip: a simplified method for Agrobacterium-mediated transformation of Arabidopsis thaliana. *Plant J.* **16**, 735–743.

Denancé, N., Szurek, B. and Noël, L.D. (2014) Emerging Functions of Nodulin-Like Proteins in Non-Nodulating Plant Species. *Plant Cell Physiol.* **55**, 469–474.

Epp, J.B., Alexander, A.L., Balko, T.W. *et al.* (2016) The discovery of Arylex™ active and Rinskor™ active: Two novel auxin herbicides. *Bioorg. Med. Chem.* **24**, 362–371.

Evans, C.E. and Norris, L.A. (1986) Picloram stability in a sample of forest soil during handling and storage. *Bull. Environ. Contam. Toxicol.* **37**, 496–500.

Fan, S.C., Lin, C.S., Hsu, P.K., Lin, S.H. and Tsay, Y.F. (2009) The Arabidopsis nitrate transporter NRT1.7, expressed in phloem, is responsible for source-to-sink remobilization of nitrate. *Plant Cell*, **21**, 2750–2761.

Grossmann, K., Kwiatkowski, J. and Tresch, S. (2001) Auxin herbicides induce H_2O_2 overproduction and tissue damage in cleavers (Galium aparine L.). *J. Exp. Bot.* **52**, 1811–1816.

Hagen, G. and Guilfoyle, T. (2002) Auxin-responsive gene expression: genes, promoters and regulatory factors. *Plant Mol. Biol.* **49**, 373–385.

Haydon, M.J. and Cobbett, C.S. (2007) A novel major facilitator superfamily protein at the tonoplast influences zinc tolerance and accumulation in Arabidopsis. *Plant Physiol.* **143**, 1705–1719.

Hori, K. and Watanabe, Y. (2005) UPF3 suppresses aberrant spliced mRNA in Arabidopsis. *Plant J.* **43**, 530–540.

Ito, H. and Gray, W.M. (2006) A gain-of-function mutation in the Arabidopsis pleiotropic drug resistance transporter PDR9 confers resistance to auxinic herbicides. *Plant Physiol.* **142**, 63–74.

Jayaweera, T., Siriwardana, C., Dharmasiri, S., Quint, M., Gray, W.M. and Dharmasiri, N. (2014) Alternative splicing of Arabidopsis IBR5 pre-mRNA generates two IBR5 isoforms with distinct and overlapping functions. *PLoS ONE*, **9**, e102301.

Johnsen, T.N. (1980) Picloram in water and soil from a semiarid Pinyon-Juniper watershed. *J. Environ. Qual.* **9**, 601–605.

© 2019 The Authors

Kanno, Y., Hanada, A., Chiba, Y., Ichikawa, T., Nakazawa, M., Matsui, M., Koshiba, T., Kmiya, Y. and Seo, M. (2012) Identification of an abscisic acid transporter by functional screening using the receptor complex as a sensor. *Proc. Natl Acad. Sci. USA*, **109**, 9653–9658.

Kim, Y.S., Schumaker, K.S. and Zhu, J.K. (2006) In EMS mutagenesis in Arabidopsis.In *Arabidopsis Protocols*. (Salinas, J. and Sanchez-Serrano, J. J., eds). New York: Springer, pp. 101–103.

Krieg, P.A. and Melton, D.A. (1984) Functional messenger RNAs are produced by SP6 in vitro transcription of cloned cDNAs. *Nucleic Acids Res.* **12**, 7057–7070.

Krouk, G., Crawford, N.M., Coruzzi, G.M. and Tsay, Y.F. (2010) Nitrate signaling: adaptation to fluctuating environments. *Curr. Opin. Plant Biol.* **13**, 266–273.

Kurihara, Y., Matsui, A., Hanada, K. *et al.* (2009) Genome-wide suppression of aberrant mRNA-like noncoding RNAs by NMD in *Arabidopsis*. *Proc. Natil Acad. Sci. USA*, **106**, 2453–2458.

Leran, S., Varala, K., Boyer, J.C. *et al.* (2014) A unified nomenclature of NITRATE TRANSPORTER 1/PEPTIDE TRANSPORTER family members in plants. *Trends Plant Sci.* **19**, 5–9.

Li, J.Y., Fu, Y.L., Pike, S.M. *et al.* (2010) The Arabidopsis nitrate transporter NRT1.8 functions in nitrate removal from the xylem sap and mediates cadmium tolerance. *Plant Cell,* **22**, 1633–1646.

Lin, S.H., Kuo, H.F., Canivenc, G. *et al.* (2008) Mutation of the Arabidopsis NRT1.5 nitrate transporter causes defective root-to-shoot nitrate transport. *Plant Cell,* **20**, 2514–2528.

Lincoln, C., Britton, J.H. and Estelle, M. (1990) Growth and development of the axr1 mutants of Arabidopsis. *Plant Cell,* **2**, 1071–1080.

Marger, M.D. and Saier, M.H. (1993) A major superfamily of transmembrane facilitators that catalyse uniport, symport and antiport. *Trends Biochem. Sci.* **18**, 13–20.

McSteen, P. (2010) Auxin and monocot development. *Cold Spring Harb. Perspect. Biol.* **2**, a001479.

Mithila, J., Hall, J.C., Johnson, W.G., Kelley, K.B. and Riechers, D.E. (2011) Evolution of resistance to auxinic herbicides: Historical perspectives, mechanisms of resistance, and implications for broadleaf weed management in agronomic crops. *Weed Sci.* **59**, 445–457.

Nelson, B.K., Cai, X. and Nebenführ, A. (2007) A multicolored set of in vivo organelle markers for co-localization studies in Arabidopsis and other plants. *Plant J.* **51**, 1126–1136.

Pao, S.S., Paulsen, I.T. and Saier, M.H. (1998) Major facilitator superfamily. *Microbiol. Mol. Biol. Rev.* **62**, 1–34.

Parry, G., Ward, S., Cernac, A., Dharmasiri, S. and Estelle, M. (2006) The Arabidopsis SUPPRESSOR OF AUXIN RESISTANCE proteins are nucleoporins with an important role in hormone signaling and development. *Plant Cell,* **18**, 1590–15603.

Peng, H., Han, S., Luo, M., Gao, J., Liu, X. and Zhao, M. (2011) Roles of multidrug transporters of MFS in plant stress responses. *Int. J. Biosci. Biochem. Bioinforma.* **1**, 109–113.

Prigge, M.J., Greenham, K., Zhang, Y., Santner, A., Castillejo, C., Mutka, A.M., O'Malley, R.C., Ecker, J.R., Kunkel, B.N. and Estelle, M. (2016) The Arabidopsis auxin receptor F-Box proteins AFB4 and AFB5 are required for response to the synthetic auxin picloram. *G3: Genes - Genomes - Genetics.* **6**, 1383–1390.

Rayson, S., Arciga-Reyes, L., Wootton, L., De Torres Zabala, M., Truman, W., Graham, N., Grant, M. and Davies, B. (2012) A role for nonsense-mediated mRNA decay in plants: pathogen responses are induced in Arabidopsis thaliana NMD mutants. *PLoS ONE*, **7**, e31917.

Reinders, A., Panshyshyn, J.A. and Ward, J.M. (2005) Analysis of transport activity of Arabidopsis sugar alcohol permease homolog AtPLT5. *J. Biol. Chem.* **280**, 1594–1602.

Remans, T., Nacry, P., Pervent, M., Girin, T., Tillard, P., Lepetit, M. and Gojon, A. (2006) A central role for the Nitrate Transporter NRT2.1 in the integrated morphological and physiological responses of the root system to nitrogen limitation in Arabidopsis. *Plant Physiol.* **140**, 909–921.

Remy, E., Cabrito, T.R., Baster, P., Batista, R.A., Teixeira, M.C., Friml, J., Sa-Correia, I. and Duque, P. (2013) A major facilitator superfamily transporter plays a dual role in polar auxin transport and drought stress tolerance in Arabidopsis. *Plant Cell*, **25**, 901–926.

Ricachenevsky, F.K., Sperotto, R.A., Menguer, P.K., Sperb, E.R., Lopes, K.L. and Fett, J.P. (2011) ZINC-INDUCED FACILITATOR-LIKE family in plants: lineage-specific expansion in monocotyledons and conserved genomic and expression features among rice (Oryza sativa) paralogs. *BMC Plant Biol.* **11**, 20.

Ruzicka, K., Strader, L.C., Bailly, A. *et al.* (2010) Arabidopsis PIS1 encodes the ABCG37 transporter of auxinic compounds including the auxin precursor indole-3-butyric acid. *Proc. Natl Acad. Sci. USA*, **107**, 10749–10753.

Sanchez, D.A., Szynkiewicz, A. and Faiia, A.M. (2017) Determining sources of nitrate in the semi-arid Rio Grande using nitrogen and oxygen isotopes. *Appl. Geochem.* **86**, 59–69.

Smith, A.E., Walte, D., Grover, R., Kerr, L.A., Milward, J. and Sommerstad, H. (1988) Persistence and movement of picloram in a northern Saskatchewan watershed. *J. Environ. Qual.* **17**, 262–268.

Vincill, E.D., Szczyglowski, K. and Roberts, D.M. (2005) GmN70 and LjN70. Anion Transporters of the Symbiosome Membrane of Nodules with a Transport Preference for Nitrate. *Plant Physiol.* **137**, 1435–1444.

Walsh, T.A., Neal, R., Merlo, A.O., Honma, M., Hicks, G.R., Wolff, K., Matsumura, W. and Davies, J.P. (2006) Mutations in an auxin receptor homolog AFB5 and in SGT1b confer resistance to synthetic picolinate auxins and not to 2,4-dichlorophenoxyacetic acid or indole-3-acetic acid in Arabidopsis. *Plant Physiol.* **142**, 542–552.

Wang, Y.Y. and Tsay, Y.F. (2011) Arabidopsis nitrate transporter NRT1.9 is important in phloem nitrate transport. *Plant Cell*, **23**, 1945–1957.

Wang, R., Okomoto, M., Xing, X. and Crawford, N.M. (2003) Microarray analysis of the nitrate response in Arabidopsis roots and shoots reveals over 1,000 rapidly responding genes and new linkages to glucose, trehalose-6-phosphate, iron, and sulfate metabolism. *Plant Physiol.* **132**, 556–567.

© 2019 The Authors
The Plant Journal © 2019 John Wiley & Sons Ltd,